NJC

New Journal of Chemistry

A journal for new directions in chemistry

Accepted Manuscript

This article can be cited before page numbers have been issued, to do this please use: P. MADHU, S. Ponnusamy and R. Sribalan, *New J. Chem.*, 2019, DOI: 10.1039/C9NJ02655J.

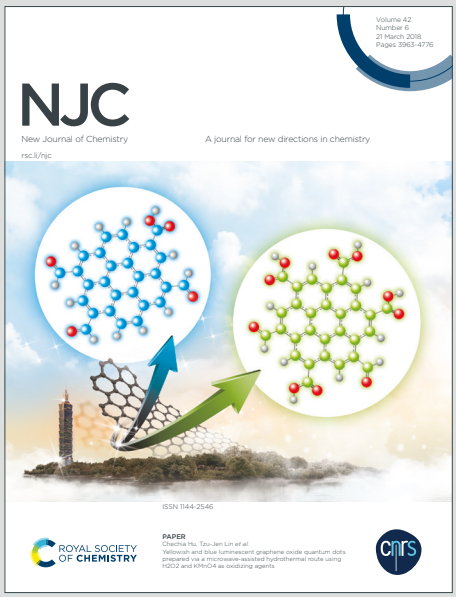

This is an Accepted Manuscript, which has been through the Royal Society of Chemistry peer review process and has been accepted for publication.

Accepted Manuscripts are published online shortly after acceptance, before technical editing, formatting and proof reading. Using this free service, authors can make their results available to the community, in citable form, before we publish the edited article. We will replace this Accepted Manuscript with the edited and formatted Advance Article as soon as it is available.

You can find more information about Accepted Manuscripts in the Information for Authors.

Please note that technical editing may introduce minor changes to the text and/or graphics, which may alter content. The journal's standard Terms & Conditions and the Ethical guidelines still apply. In no event shall the Royal Society of Chemistry be held responsible for any errors or omissions in this Accepted Manuscript or any consequences arising from the use of any information it contains.

View Article Online
DOI: 10.1039/C9NJ02655J

Benzofuran-*β*-alaninamide based "turn-on" fluorescent chemosensor for selective recognition of Fe^{3+} ions

P. Madhu[a,b,*], P. Sivakumar[c] and Rajendran Sribalan[d]

[a]*Research and Development Centre, Bharathiar University, Coimbatore-641 046, TamilNadu, India*

[b]*Department of Chemistry, Thiruvalluvar Government Arts College, Rasipuram-637 401, TamilNadu, India*

[c]*Department of Chemistry, Arignar Anna Government Arts College, Namakkal-637 002, TamilNadu, India*

[d]*Biochemie Innovations Lab, Tindivanam-604 001, TamilNadu, India*

**Corresponding Author E-mail: madhup.chem@gmail.com*

Tel: +91 9944502310

Abstract

A benzofuran-*β*-alaninamide based chemosensor, 3-(3-((4-methylbenzyl)amino) propanamido)benzofuran-2-carboxamide (**BAA**) was designed and synthesized for selective detection of Fe^{3+} ions. The binding ability of **BAA** towards Fe^{3+} in DMSO/H_2O solution (9/1, v/v) have been studied by UV-vis absorption and fluorescence spectroscopy. Interestingly, the probe **BAA** exhibits an excellent "turn-on" fluorescence enhancement at 424 nm with the excitation wavelength of 290 nm. The quantum yield was determined to be 0.248 for **BAA** and 0.447 for the iron complex. The limit of detection (LOD) calculated to be 1.3 µM and 0.067 µM by UV-vis absorption and fluorescence methods respectively. These values are much lower than that of US, Environmental protection agency guidelines in drinking water (5.37 µM). Job's plot measurement evidenced the 2:1 binding stoichiometry for the complex formed between **BAA** and Fe^{3+}. Moreover, the binding interaction of **BAA** towards Fe^{3+} was confirmed by density functional theory (DFT) study. Finally, the real sample analysis proved that the probe **BAA** was more suitable for the detection of Fe^{3+}.

Keywords: Chemosensor; Fluorescent sensor; benzofuran-*β*-alaninamide sensor; Fe^{3+} ion; DFT study.

Introduction

In recent years, the research on chemosensors for environmentally and physiologically important analytes have attracted immense interests to chemists, biologists due to their potential

View Article Online
DOI: 10.1039/C9NJ02655J

applications in the field of biological, clinical and environmental systems.[1-3] Iron is one of the most abundant and indispensable transition metal ions in biological systems and plays a vital role in many biochemical processes such as cellular metabolism, DNA synthesis, transport of oxygen by heme and cofactor in many enzymatic reactions.[4,5] The iron-rich organs in the human body are liver and spleen. It is also present in bones, medulla, kidneys and intestines in smaller amounts.[6] Although iron is a very essential element for the proper functioning of living cells, the deficiency and excess may cause series effects in the human body. The deficiency of iron causes many biological disorders such as anemia, liver damage, cancer and decreased immunity.[7,8] At the same time, the excess of iron produces reactive oxygen species (ROS) by Fenton reaction, which damages proteins, lipids and nucleic acids.[9-14] Moreover, hemochromatosis is characterized by an overload of iron in the body that causes tissue damage and fibrosis with irreversible damage to various organs.[15,16] Recently researchers revealed that iron accumulation in the brain has been associated with Parkinson's disease, Alzheimer's disease and Huntington's chorea.[17-24] Thus, an urge to develop a new sensitive method for direct sensing of iron in the living system and environmental samples are of great scientific interest.

Numerous analytical techniques such as atomic absorption spectroscopy,[25] spectrophotometry,[26] inductively coupled plasma mass spectroscopy,[27] anodic stripping voltammetry,[28] neutron activation analysis,[29] electrothermal atomic absorption spectrometry,[30] atomic fluorescence spectrometry,[31] X-ray fluorescence spectrometry[32] and cold vapour atomic absorption spectrometry[33] have been used for the detection of iron ions, but these methods have some disadvantages such as being expensive, requirement of sophisticated instruments, limited sample adaptability and necessity of professional operators.[34] Thus, the chemosensors are of a good choice and alternative technique for the detection of metal ions, which include high sensitivity, good selectivity, cost-effectiveness, rapidity, easy monitoring the analyte, visual perception and applicability to the environmental and biological milieus. Although a number of fluorescence based chemosensors have been developed and reported for various transition metals,[35-37] only a few fluorescent probes were reported for Fe^{3+} ions. As Fe^{3+} known to be paramagnetic nature, most of the reported iron sensors exhibited fluorescence quenching responses,[38-40] only in few cases fluorescence enhancement was observed. Thus, there is an instant requirement to develop "turn-on" fluorescent chemosensors that are capable of detecting Fe^{3+} ions in biological and environmental samples.

View Article Online
DOI: 10.1039/C9NJ02655J

A number of bioactive natural products, as well as pharmaceuticals and polymers, contains benzofuran moiety.[41] Many of these benzofuran derivatives are found to be biologically active.[42-58] Thus, herein we developed a benzofuran-*β*-alaninamide based chemosensor for selective detection of Fe^{3+} ions in the presence of other metal ions. The sensor showed "turn-on" fluorescence response with high selectivity and sensitivity towards Fe^{3+} ions in DMSO/H_2O solution (9:1, v/v).

Experimental

Materials and Instrumentation

All the chemicals and solvents were purchased from Sigma-Aldrich/Merck with analytical and spectroscopic grade and used as received without further purification. The progression of all the reactions monitored by TLC using silica gel 60F254 and visualized under UV 254-366 nm and iodine.

Bruker NMR instrument was used to record ^{1}H NMR (300MHz) and ^{13}C NMR (75MHz) in $CDCl_3$ and DMSO-D_6 as solvents. LCQ Fleet mass spectrometer (Thermo Fisher Instruments Ltd., US) was used to record Electrospray ionization mass spectra (ESI-MS). FT-IR spectra were recorded on Thermo Scientific Nicolet iS50 FT-IR Spectrometer. For recording the FT-IR spectrum of the metal complex, the probe, **BBA** and Fe^{3+} solutions were mixed, dried at room temperature and the powder sample obtained was used. Shimadzu UV-1800 and JASCO V-630 UV-vis spectrophotometers and fluorescence spectrophotometers (Agilent Technologies, US and JASCO F-8500) were used to record UV absorption and Fluorescence spectra respectively.

Synthesis and characterization

Synthesis of 2-(cyanomethoxy)benzonitrile(2)[59]

2-hydroxybenzonitrile (0.00839mol) **1** was dissolved in DMF solution and stirred at room temperature. Then potassium carbonate (0.0125mol) and 2-chloroacetonitrile (0.00839mol) was added to the reaction mixture. The resulting solution was refluxed to 80°C for 3h. After completion of the reaction, the reaction mixture was poured into cold water and filtered. The obtained solid was washed with traces amount of hexane and then dried to get compound **2**. Brown solid. Yield 88%. ^{1}H NMR ($CDCl_3$, 300 MHz): δ 7.62-7.68 (m, 2H), 7.11-7.23 (m, 2H), 4.94 (s, 2H). ^{13}C NMR ($CDCl_3$, 75 MHz): δ 157.66, 134.72, 134.44, 123.36, 115.47, 114.20, 112.55, 102.96, 53.90.

View Article Online
DOI: 10.1039/C9NJ02655J

*Synthesis of 3-aminobenzofuran-2-carboxamide (**3**)* [59]

2-(cyanomethoxy)benzonitrile (0.00632 mol) **2** was dissolved in 100mL of ethanol and KOH (0.00948 mol) was added. The reaction mixture was refluxed to 75°C for 3 h. Then the reaction mixture was poured into the crushed ice, filtered and dried. The obtained solid was dried to afford compound **3**. White solid. Yield 68%. ^{1}H NMR ($CDCl_3$, 300 MHz): δ 7.45 (d, *J* = 9.0 Hz, 1H), 7.35-7.40 (m, 2H), 7.26 (d, *J* = 9.0Hz, 1H), 5.97 (s, 2H), 5.06 (s, 2H). ^{13}C NMR ($CDCl_3$, 75 MHz): δ 162.91, 151.85, 135.66, 126.82, 125.80, 121.80, 121.02, 119.82, 110.73.

*Synthesis of 3-(3-((4-methylbenzyl)amino)propanamido)benzofuran-2-carboxamide (**BAA**)*[59]

The compound **3** (0.00368mol) was dissolved in acetonitrile. Then triethylamine (0.00552mol) was added at 0–5°C. To that solution, 3-chloropropionyl chloride (0.00368mol) was added drop wise over 5 min. And then 4-methylbenzylamine (0.00368mol) was added at ambient temperature for 6 h. Then the reaction mixture was diluted with dichloromethane (50 mL), washed with water (2-25 mL) and brine solution (25 mL). The organic layer was dried over anhydrous sodium sulphate, filtered and evaporated to obtain **BAA**. White solid. Yield 73%. ^{1}H NMR ($CDCl_3$, 300 MHz): δ 10.45 (s, 1H), 8.34 (d, *J* = 8.1 Hz, 1H), 7.39-7.45 (m, 2H),7.28-7.30 (m,1H), 7.23 (d, *J* = 7.8Hz, 2H), 7.12 (d, *J* = 7.8 Hz, 2H), 7.10 (s, 1H), 5.78 (s, 1H), 3.85 (s, 2H), 3.04 (t, *J* = 6.0 Hz, 2H), 2.69 (t, *J* = 6.0 Hz, 2H), 2.32 (s, 3H). ^{13}C NMR (DMSO-d_6, 75 MHz): δ 170.72, 163.01, 153.42, 136.78, 136.70, 132.28, 129.20, 128.27, 128.20, 126.73, 123.19, 122.36, 111.62, 53.44, 44.71, 36.95, 21.14. FT-IR (KBr) cm^{-1}; 3378, 3299, 3169, 2968, 1670, 1600, 859, 748. ESI-MS calculated, 351.1; found 352.3$(M+1)^+$ and 350.2 $(M-1)^-$. Anal. Calcd for: $C_{20}H_{21}N_3O_3$.: C, 68.36; H, 6.02; N, 11.96 %. Found: C, 68.38; H, 6.01; N, 11.94 %.

UV-vis and fluorescence spectral studies

The solvent optimization was performed with increasing ratio of DMSO/water and found best at 9/1 (Fig. S16 and Fig. S17). The **BAA** was dissolved in DMSO/H_2O solution (9/1, v/v) and prepared at a concentration of 1 x 10^{-3} M and kept as a stock solution. 50 µL of this stock solution was diluted to 2 mL with the respective solvent system to cover final concentration as in 25 µM level. The stock solution of metal ion was prepared at a concentration of 1 x 10^{-2} M and 10 equiv. of this solution was used for the selectivity experiments. This stock solution was diluted (10 times) for the sensitivity experiments. For job's plot analysis 5 x 10^{-5} M of **BAA** and

View Article Online
DOI: 10.1039/C9NJ02655J

Fe^{3+} solutions were used as a separate solution. In competitive experiments, 25 μM concentration of **BAA**, 10 equiv. of Fe^{3+} and 15 equiv. of other metal ions were used. Freshly prepared solutions of **BAA** and metal solutions were used for the purpose of spectral measurements.

UV-vis spectrophotometer and fluorescence spectrophotometer were used to record the absorption and fluorescence spectra at room temperature respectively. 25 μM solution of **BAA** in DMSO/H_2O solution (9/1, v/v) at a pH range of 9.0 was prepared at room temperature and added to the metal ions. This solution was taken in quartz optical cell and the spectra were recorded. The emission spectral studies were performed on fluorescence spectrophotometer and the **BAA** shows a broad band centered at 376 nm with the excitation wavelength of 290 nm.

Binding constant

The binding constant for (K) the formation of the complex was evaluated by UV-vis and Fluorescence Spectrophotometer. The binding constant value can be determined by UV-vis spectrophotometer by using the Benesi-Hildebrand equation stated below,

$$\frac{1}{A - A_0} = \frac{1}{K_a\,(A_{max} - A_0)\,[Fe^{3+}]} + \frac{1}{A_{max} - A_0} \quad \text{------- (1)}$$

Where, A is the absorbance recorded in the presence of added Fe^{3+} ions, A_o is the absorbance of the receptor, **BAA** in the absence of guest Fe^{3+}, A_{max} is absorbance in presence of added $[Fe^{3+}]_{max}$ and K is the binding constant (M^{-1}). The binding constant has been determined from the slope of the straight line obtained in the plot of $1/(A-A_o)$ against $1/[Fe^{3+}]$. By the same manner, the binding constant value can also be determined by fluorescence spectrophotometer by using modified Benesi-Hildebrand equation stated below,

$$\frac{1}{I - I_{min}} = \frac{1}{I_{max} - I_{min}} + \frac{1}{K\,[Fe^{3+}]} \frac{1}{I_{max} - I_{min}} \text{------ (2)}$$

Here, I_{min}, I and I_{max} are the emission intensities of **BAA**, at an intermediate Fe^{3+} concentration with **BAA**, and at a concentration of complete saturation respectively. K is the binding constant and $[Fe^{3+}]$ is the concentration of Fe^{3+}ions. From the plot of $1/(I-I_{min})$ against $[Fe^{3+}]^{-1}$, the binding constant has been determined.

Computational methods

Using Gaussian 09W program, all the energy optimized structure calculations were carried out. The geometry of the energy optimized structures of **BAA** and the iron complex in

View Article Online
DOI: 10.1039/C9NJ02655J

the ground state and excited state were performed by using density functional theory (DFT) method with the B3LYP/6.311++G(d,p) basis set and LANL2DZ level.

Results and discussion

Synthesis and structural characterization of **BAA**

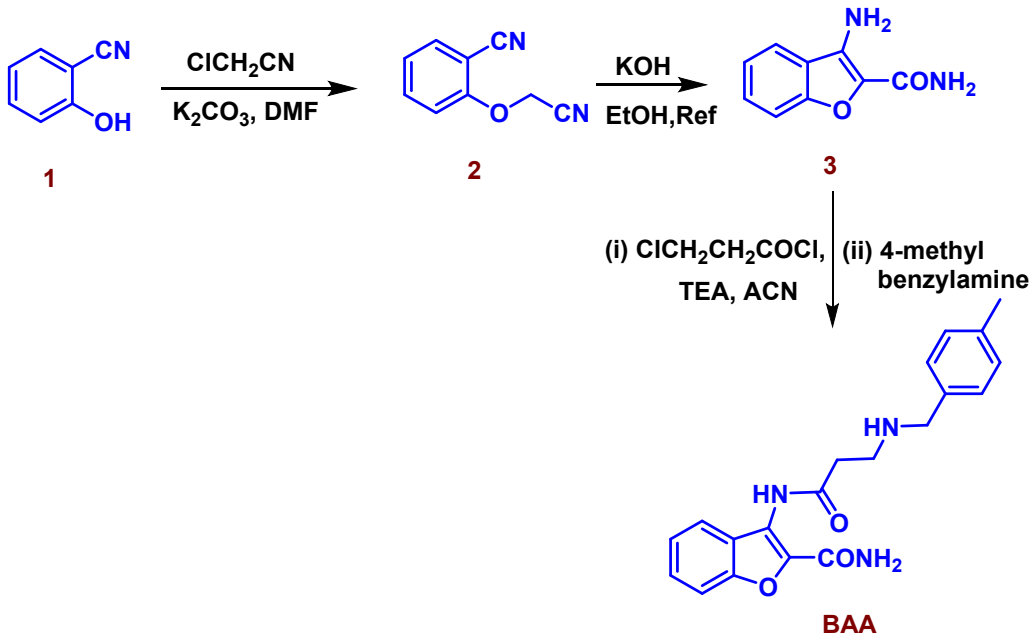

Scheme 1. Synthetic route of **BAA**

As shown in Scheme 1, the **BAA** was successfully synthesized from 2-hydroxybenzonitrile. Initially, 2-hydroxybenzonitrile reacts with 2-chloroacetonitrile in the presence of potassium carbonate yielded intermediate **2**. The intermediate **3** was obtained from the internal cyclization of intermediate **2** in the presence of potassium hydroxide. The **BAA** was obtained from compound **3** with the coupling of 3-chloropropanoyl chloride followed by the nucleophilic substitution with 4-methylbenzylamine. The structure of **BAA** was satisfactorily characterized by using ^{1}H NMR, ^{13}C NMR, ESI-MS and FT-IR spectroscopic techniques. In ^{1}H NMR, the appearance of singlet at 10.45 ppm indicates the presence of secondary amide NH. Similarly, the singlet around 6.4 and 5.7 ppm indicates the presence of primary amide NH_2. The appearance of sharp singlet at 2.32 and 3.84 ppm indicates the presence of methyl protons and

View Article Online
DOI: 10.1039/C9NJ02655J

methylene protons of the *p*-tolylmethanamine unit. The set of triplets at 2.69 and 3.03 ppm indicates the presence of methylene protons of alaninamide moiety. The remaining aromatic protons appeared in their corresponding chemical shifts. The ^{13}C NMR spectrum also confirms the product formation. The peaks around 170.72 and 162.01 ppm indicate the presence of primary and secondary amide carbonyl units. The appearance of carbon signals 21.12 and 53.44 ppm indicates the presence of tolylmethyl and benzyl methylene units. The peaks at 36.95 ppm and 44.71 ppm indicate the presence of alaninamide methylene units. The Mass spectrum clearly showed a molecular ion peak at both positive and negative mode. The FT-IR spectrum gave some additional information for the compound formation. The stretching vibration at 3169 cm^{-1} and 2958 cm^{-1} were appeared due to the presence of aromatic CH units. The band at 3299 cm^{-1} and 3378 cm^{-1} indicate the presence of amide NH and amine NH units. The strong absorption band at 1600 cm^{-1} and 1670 cm^{-1} showed the compound contains the amide carbonyl units.

Selectivity of **BAA** for Fe^{3+} detection

Various biologically relevant metal ions were used to investigate the selectivity and binding nature of the probe **BAA**. Initially, the synthesized probe **BAA** (25 μM) in DMSO/H_2O solution (9/1, v/v) shows an absorption maximum at 298 nm in UV-vis spectroscopy. Upon addition of 10 equiv. of various metal ions such as Zn^{2+}, Cd^{2+}, Hg^{2+}, Pb^{2+}, Cu^{2+}, Ni^{2+}, Co^{2+}, Fe^{2+}, Fe^{3+}, Mn^{2+}, Mg^{2+}, Ba^{2+} and Ca^{2+} no significant changes were observed except Fe^{3+} ions. Trivalent metal ions such as Mn^{3+}, Co^{3+}, Cr^{3+} and Al^{3+} also does not influences the absorbance of the probe, **BBA** (Fig. S10). As shown in Fig.1, the addition of Fe^{3+} to the probe **BAA**, the absorption band at 298 nm gradually increased, indicating that the probe **BAA** selectively bind with Fe^{3+} ion in DMSO/H_2O solution (9/1, v/v).

To get more evidence for the selectivity of **BAA** for metal ions, the fluorescence intensity was measured upon the addition of 10 equiv. of different metal ions such as Zn^{2+}, Cd^{2+}, Hg^{2+}, Pb^{2+}, Cu^{2+}, Ni^{2+}, Co^{2+}, Fe^{2+}, Fe^{3+}, Mn^{2+}, Mg^{2+}, Ba^{2+} and Ca^{2+} using fluorescence spectrophotometer under identical conditions (Fig.2). The probe **BAA** (25 μM) in DMSO/H_2O solution (9/1, v/v) exhibit a broad fluorescence band at 376 nm with the excitation wavelength of 290 nm. Upon addition of Fe^{3+} ion, the emission intensity of **BAA** at 376 nm decreased and a significant fluorescence enhancement at 424 nm emerged quickly, while other metal ions did not induce any distinct spectral changes in fluorescence spectroscopy. Also, trivalent metal ions

View Article Online
DOI: 10.1039/C9NJ02655J

such as Mn^{3+}, Co^{3+}, Cr^{3+} and Al^{3+} did not show any significant changes (Fig. S11). This drastic fluorescent enhancement revealed that the probe **BAA** strongly binds with Fe^{3+} ion. The quantum yield (Φ) of **BAA** and the iron complex were found to be 0.248 and 0.447 respectively. These results suggest that the **BAA** has superior selectivity towards Fe^{3+} over other metal ions.

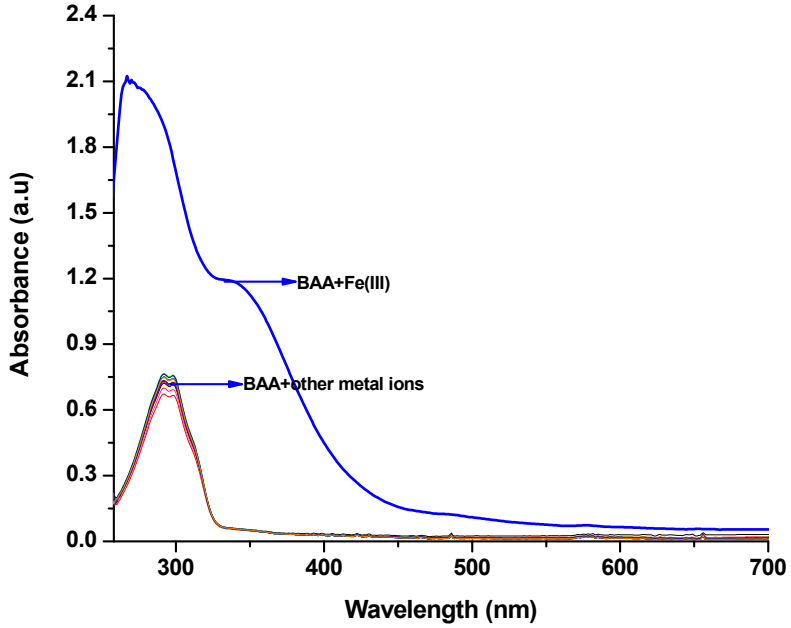

Fig. 1 UV-vis spectra of **BAA** (25 μM) with 10 equiv. of various metal ions in DMSO/H_2O solution (9:1, v/v).

View Article Online
DOI: 10.1039/C9NJ02655J

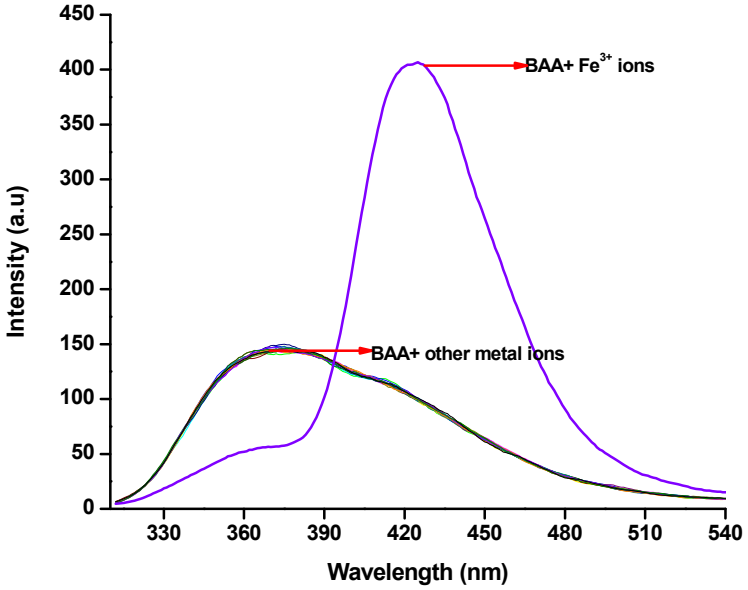

Fig. 2 Fluorescence spectra of **BAA** (25 μM) with 10 equiv. of various metal ions in DMSO/H_2O solution (9:1, v/v).

Sensitivityof **BAA** for Fe^{3+} detection

The sensitivity of **BAA** with Fe^{3+} ion was interrogated by the absorption spectral titration in DMSO/H_2O solution (9/1, v/v). Upon the addition of Fe^{3+} ion from 0-250 μM to **BAA,** a new increment of absorbance was observed at 338 nm as shown in Fig.3. This study clearly shows that the **BAA** has good linearity having a linear coefficient of 0.99. The detection limit of **BAA** for Fe^{3+} was found to be 1.3 μM (Fig. S12). This value is much lower than the previously reported literature (Table 1). The linear range of chemosensor is found to be in the range of 1-19 x 10^{-5} M. Using the Benesi-Hildebrandplot,[60] the binding constant value (K) of **BAA** with Fe^{3+} was calculated to be 0.625 x 10^2 M^{-1} (Fig. S13). From the Job's plot experiment,[61-63] the binding stoichiometry between **BAA** and Fe^{3+} was confirmed to be 2:1 (Fig. 4).

View Article Online
DOI: 10.1039/C9NJ02655J

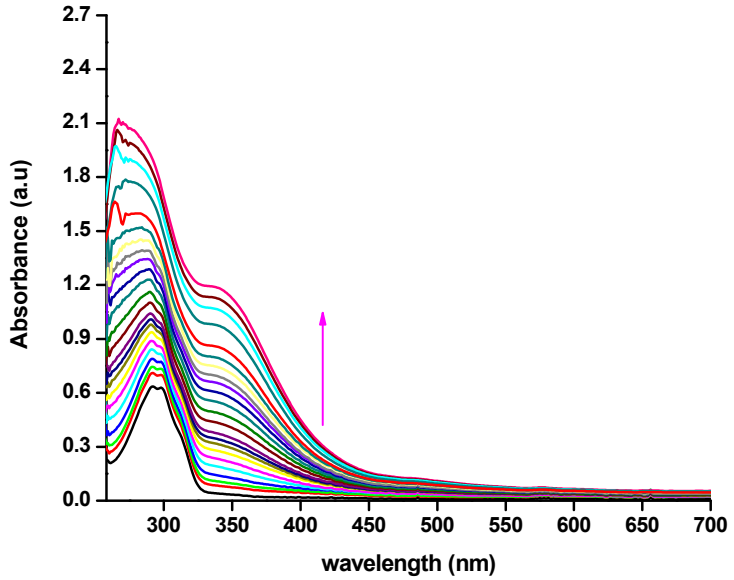

Fig. 3 UV-vis spectra of **BAA** (25 μM) with increasing concentration of the Fe^{3+} ions in DMSO/H_2O solution (9:1, v/v).

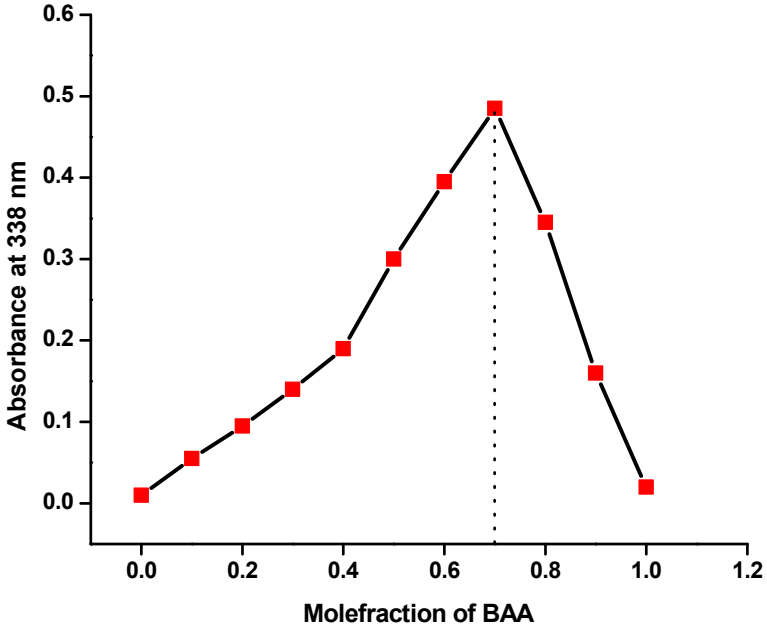

Fig. 4 Job's plot for the stoichiometry determination of **BAA** and Fe^{3+} in the complexation

View Article Online
DOI: 10.1039/C9NJ02655J

Table 1

Comparison of the detection limit for Fe^{3+} between the present study and those previously reported in the literature by UV-vis titration method.

Sensor	Target	Detection limit (μM)	References
Magnesium oxide nanoparticles	Fe^{3+}	23.00	66
Coumarin schiff based chemosensor	Fe^{3+}	5.38	67
Aldazine-based chemosensors	Fe^{3+}	9.50	68
Coumarin schiffbase derivative	Fe^{3+}	1.79	69
Benzofuran-*β*-alaninamide based chemosensor	Fe^{3+}	1.30	This study

Further to define the sensitive interaction between the **BAA** and Fe^{3+}, the fluorescence spectral titration was performed in DMSO/H_2O solution (9/1, v/v) (Fig. 5). Before the addition of Fe^{3+} ion, **BAA** exhibited fluorescence emission at 376 nm attributed to internal charge transfer (ICT) process. Upon addition of Fe^{3+} ion from 0-60 μM, the emission intensity at 376 nm was decreased and a new emission band centered at 424 nm increased with a clear isoemissive point at 393 nm. This is because the emission intensity at 376 nm was decreased due to the retardation of the ICT process[64] and a new emission band centered at 424 nm increased due to a strong chelation-enhanced fluorescence (CHEF) effect of Fe^{3+} with **BAA**. The limit of detection (LOD) of **BAA** for Fe^{3+} was calculated to be 0.067 μM based on the formula 3σ/slope (Fig. S14), which is better than the previously reported values (Table 2). Accordingly, this LOD is much lower than the upper limit of Fe^{3+} level in drinking water set by the US Environmental protection agency,[65] which is 5.37 μM. The linear range of chemosensor is found to be in the range of 2-6 x 10^{-5} M. The calculated binding constant value from the modified Benesi-Hildebrand plot was 0.089 x 10^2 M^{-1} (Fig. S15).

View Article Online
DOI: 10.1039/C9NJ02655J

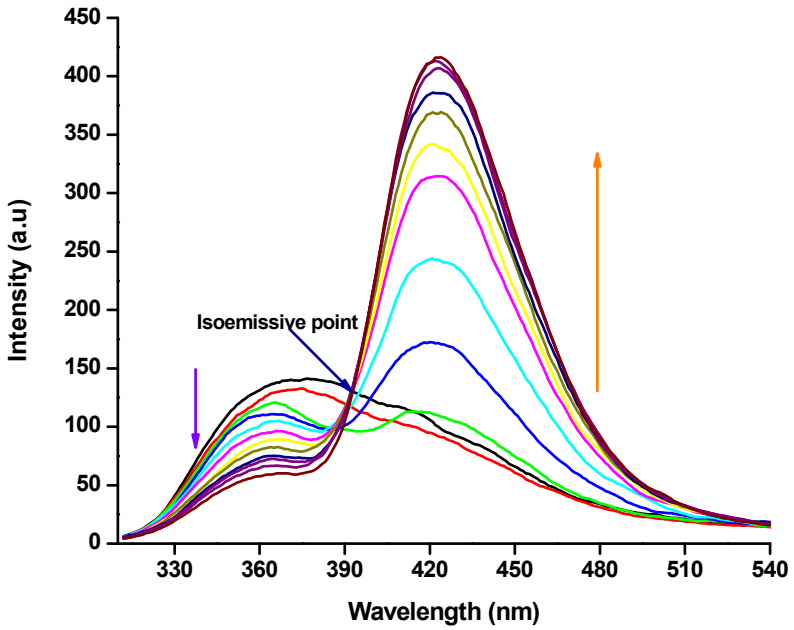

Fig. 5 Fluorescence spectra of **BAA** (25 μM) with increasing concentration of Fe^{3+} ions in DMSO/H_2O solution (9:1, v/v).

Table 2

Comparison of the detection limit for Fe^{3+} between the present study and those previously reported in the literature by fluorescence titration method.

Sensor	Target	Detection limit (μM)	References
Pyrene based chemosensor	Fe^{3+}	2.61	70
Quinoline-functionalised Schiff base	Fe^{3+}	4.00	71
Rhodamine based chemosensor	Fe^{3+}	5.05	72
Carbazole based schiff base	Fe^{3+}	2.75	73
Benzofuran-*β*-alaninamide based chemosensor	Fe^{3+}	0.067	This study

Competitive experiment

To evaluate the practical applicability of the probe **BAA** as a Fe^{3+} selective fluorescence sensor, the competitive experiment was performed in DMSO/H_2O solution (9/1, v/v) in the presence of Fe^{3+} at 10 equiv. mixed with various metal cations like Zn^{2+}, Cd^{2+}, Hg^{2+}, Pb^{2+}, Cu^{2+}, Ni^{2+}, Co^{2+}, Fe^{2+}, Fe^{3+}, Mn^{2+}, Mg^{2+}, Ba^{2+}, Ca^{2+}, Mn^{3+}, Co^{3+}, Cr^{3+} and Al^{3+} at 15 equiv. and the

View Article Online
DOI: 10.1039/C9NJ02655J

resulting individual solutions are analyzed by using UV-vis and fluorescence spectrophotometer. As shown in Fig. 6 and Fig. 7, the addition of other metal ions even in higher concentration did not show any significant spectral changes. This result showed that the **BAA** has remarkable selectivity towards Fe^{3+} and could be used as a selective chemosensor for Fe^{3+} in the presence of other metal ions.

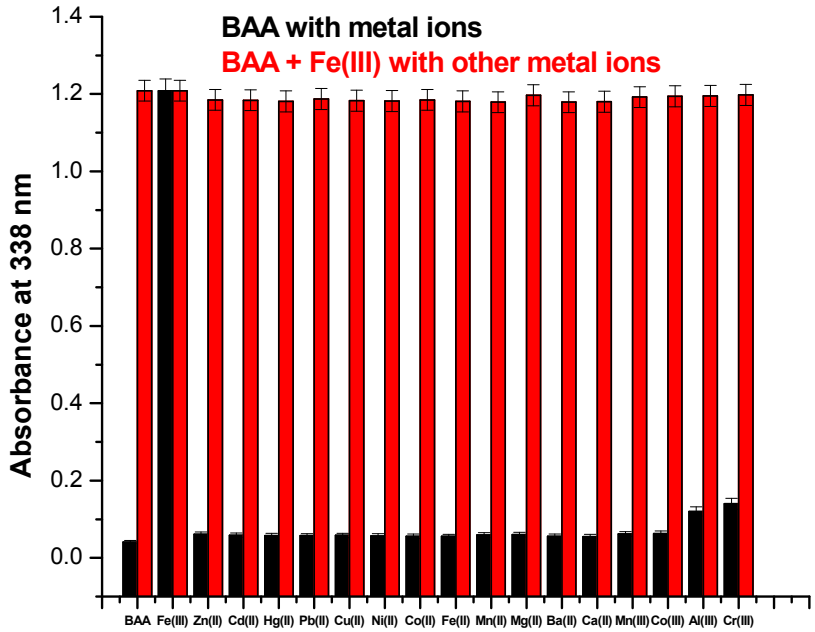

Fig. 6 Competitive experiment of **BAA** with 10 equiv. of Fe^{3+} ions and 15 equiv. of other metal ions in UV-vis spectroscopy.

View Article Online
DOI: 10.1039/C9NJ02655J

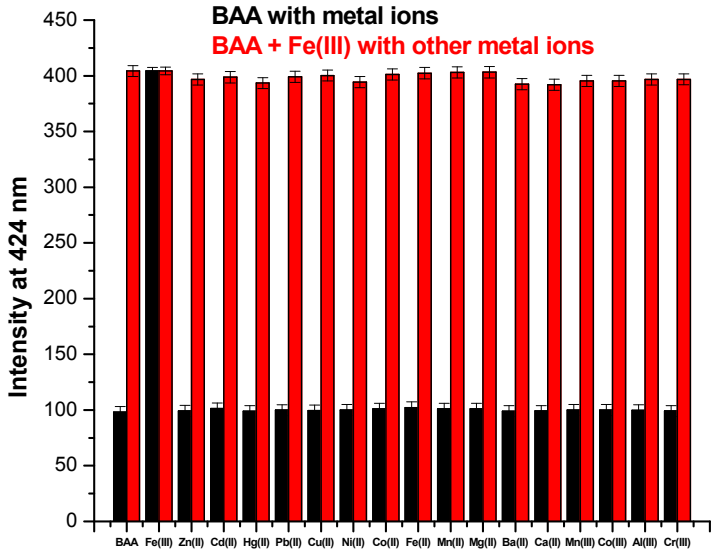

Fig. 7 Competitive experiment of **BAA** with 10 equiv. of Fe^{3+} ions and 15 equiv. of other metal ions in Fluorescence spectroscopy.

Binding reversibility

It was of immense interest to investigate the reversible binding ability of **BAA** with Fe^{3+} ion. As shown in Fig. 8, the initial fluorescence intensity of **BAA** was significantly enhanced upon the addition of 10 equiv. of Fe^{3+} ions. EDTA as a strong affinity for Fe^{3+} was introduced into the solution containing **BAA** and Fe^{3+} in the same concentration as Fe^{3+}, the fluorescence intensity was decreased immediately to the original state of **BAA**, due to a strong complex binding between EDTA and Fe^{3+}. The alternate addition of Fe^{3+} and EDTA to **BAA** "ON-OFF-ON" fluorescence signal was observed even after several cycles. These results suggested that the sensor **BAA** could be used as a reversible chemosensor for Fe^{3+}.

View Article Online
DOI: 10.1039/C9NJ02655J

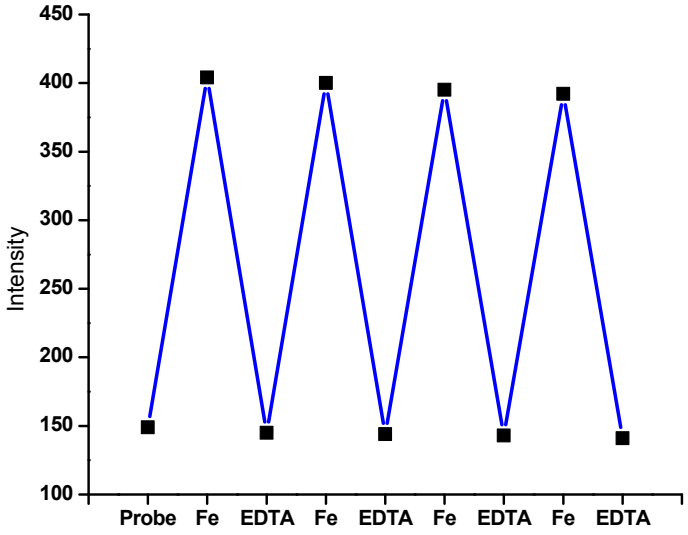

Fig. 8 Reversible fluorescence intensity changes after the sequential addition of Fe^{3+} and EDTA to **BAA**

Sensing mechanism of **BAA** with Fe^{3+}

In addition to elucidating the interaction mechanism between **BAA** and Fe^{3+}, the ^1H NMR spectral analysis of **BAA** (3.0×10^{-2} M, 2.0 equiv.) with Fe^{3+} was studied in DMSO-D_6. As shown in Fig. 9, upon addition of Fe^{3+} to **BAA**, the H_a proton signal decreased gradually and disappeared at eventually with 1.0 equiv. concentration of Fe^{3+} in ^1H NMR spectra, indicating that H_a attached carboxamide nitrogen atom was coordinated with Fe^{3+} during the complexation, whereas H_b and H_c proton signals were decreased by only 50%. This clearly signifies that 2:1 mode of binding between **BAA** and Fe^{3+}, consequently H_b proton of one molecule and H_c proton of another molecule they are coordinated with Fe^{3+}. The reason is that the protons H_b and H_c, they are not environmentally same, i.e. they exist as cis and trans in orientation with respect to –C=O group. The plausible binding interaction of Fe^{3+} with **BAA** was represented in Scheme 2.

Further to examine the sensing mechanism of the [**BAA**]$_2$-Fe^{3+}, FT-IR spectral analysis was carried out for **BAA** and [**BAA**]$_2$-Fe^{3+} complex. The FT-IR spectrum of **BAA** (Fig. S8) showed strong band at 3299 cm^{-1} and 3378 cm^{-1} corresponding to secondary amide NH and primary amide NH_2 units and these bands were shifted in the FT-IR spectrum of [**BAA**]$_2$-Fe^{3+} complex (Fig. S9), but sharp absorption band at 1600 cm^{-1} and 1670 cm^{-1} corresponding to

View Article Online
DOI: 10.1039/C9NJ02655J

amide carbonyl units remains unaffected during complexation indicating that the amide carbonyl units does not take part in any interaction with Fe^{3+}. These results suggesting that the **BAA** strongly interacted with the Fe^{3+} ions.

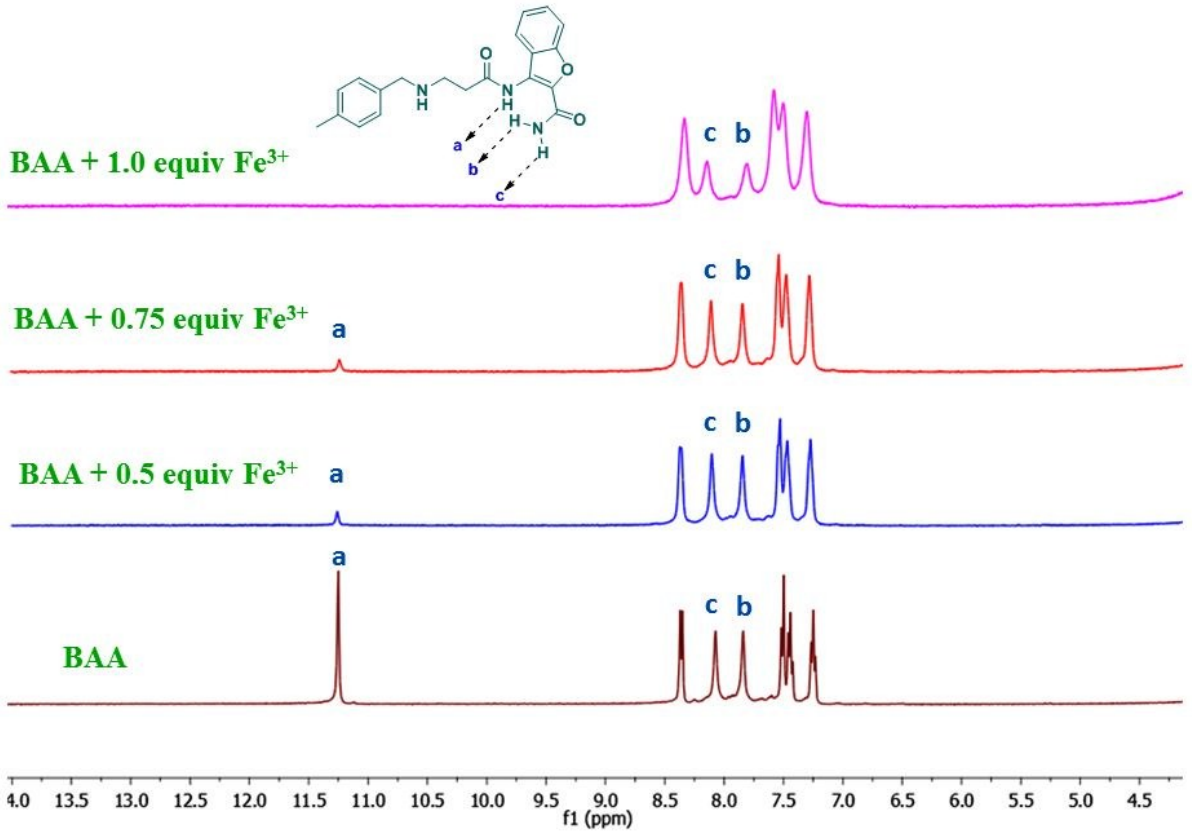

Fig. 9 ^{1}H NMR (DMSO-D_6, 400MHz) spectra of **BAA** (3.0×10^{-2} M, 2.0 equiv.) in the presence of varying amounts of Fe^{3+}.

Theoretical study

In order to get more insight into the interaction mechanism between **BAA** and Fe^{3+}, the energy optimized structure of **BAA** and $[\mathbf{BAA}]_2$-Fe^{3+} complex were obtained from density functional theory (DFT) method with B3LYP/6.311++G(d,p) and LANL2DZ level of Gaussian 09 program.

View Article Online
DOI: 10.1039/C9NJ02655J

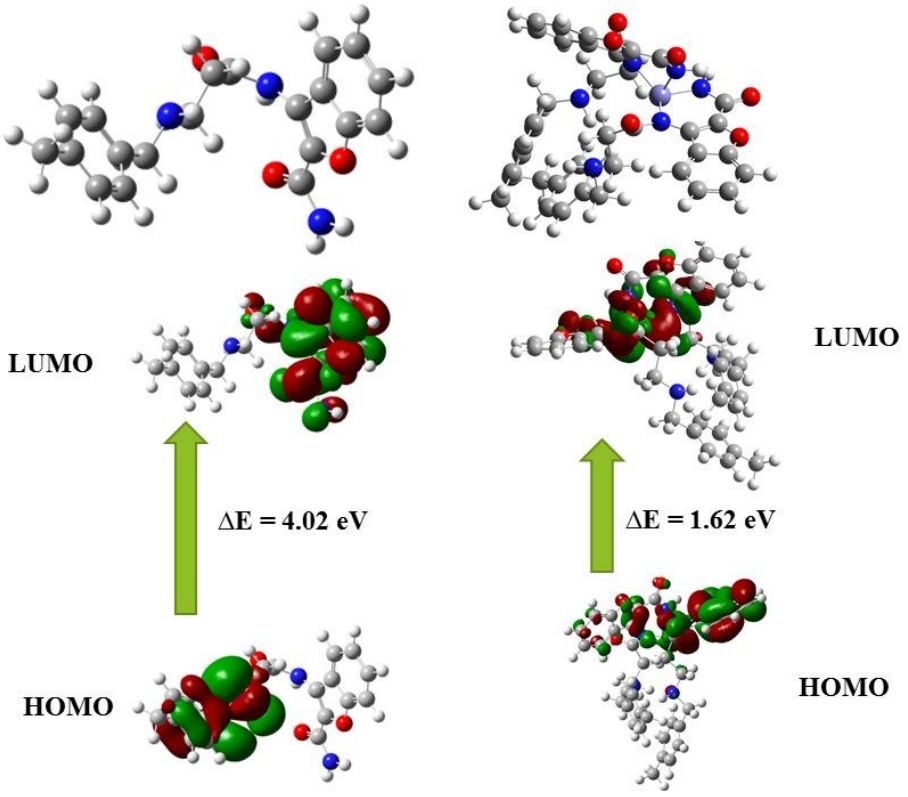

Fig. 10 DFT analysis of the **BAA** and [**BAA**]$_2$-Fe^{3+} complex (left to right).

As illustrated in Fig. 10, the probe **BAA** displays more electron density on *p*-tolylmethanamine moiety in HOMO. In LUMO, these electron densities were completely transferred into benzofurancarboxamide moiety attributed to the ICT process. After the addition of Fe^{3+} to the probe **BAA**, the electron density spread over on benzofurancarboxamide moiety and the iron environment in HOMO, whereas in LUMO the electron density was spreading over on carboxamide unit of a benzofurancarboxamide moiety, furan unit of benzofuran moiety and the iron environment. This clearly revealed that on the addition of $Fe^{3+}$to **BAA**, the ICT process was retarded and simultaneously a strong CHEF effect was tuned. Moreover, the energy gap between HOMO and LUMO of **BAA** (4.02 eV) is higher than the energy gap between HOMO and LUMO of [**BAA**]$_2$-Fe^{3+} complex (1.62 eV). Alternatively, due to the formation of [**BAA**]$_2$-Fe^{3+} complex, the energy gap between HOMO and LUMO of [**BAA**]$_2$-Fe^{3+} was decreased to 2.40 eV. The result suggests that the sensor **BAA** strongly binds with Fe^{3+} ion and form stable [**BAA**]$_2$-Fe^{3+} complex as shown in Scheme 2.

View Article Online
DOI: 10.1039/C9NJ02655J

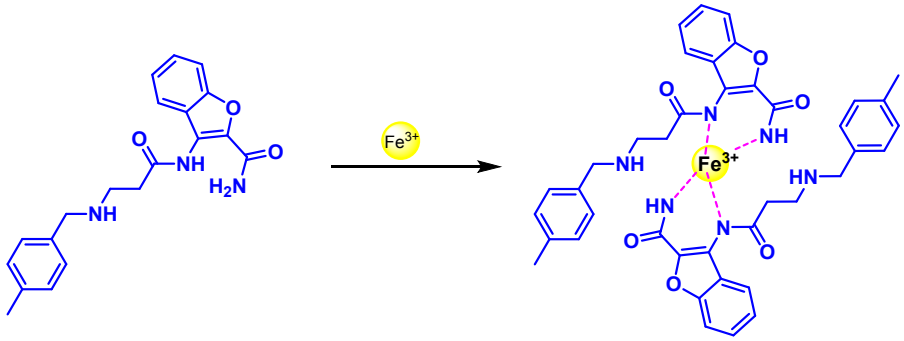

Scheme 2. Proposed sensing mechanism of **BAA** with Fe^{3+} ion.

Real sample analysis

In order to inspect the capability of the reported chemosensor in environmental samples, **BAA** was tested to detect the Fe^{3+} ion in tab water, drinking water and lake water samples in the presence of Fe^{3+} ion as previous experiments in the same concentration. As shown in Table 3, the drinking water samples showed higher absorbance than regular experimental results. Tab water showed higher absorbance than regular experimental results but slightly lower than the drinking water. In case of lake water sample, the absorbance was lower than the regular experiment. The reason is that it may contain other minerals which may interact with our probe, **BAA**. This real sample analysis proved that the **BAA** evidently detecting the Fe^{3+} in environmental water samples.

Table 3

Determination of Fe^{3+} ion in different environmental water samples

S.No.	Environmental water sample	Concentration of the Fe^{3+} added (μM)	Recovery percentage (%)	RSD (%)
1	Drinking water	25	104	6
2	Tap water	25	102	6.1
3	Lake water	25	99	5.9

Conclusion

In summary, herein we developed a benzofuran-*β*-alaninamide based chemosensor for the detection of Fe^{3+} ions. The UV-vis absorption and fluorescence spectral studies showed that the probe **BAA** acts as a highly selective and sensitive "turn-on" chemosensor for Fe^{3+} ions. The

View Article Online
DOI: 10.1039/C9NJ02655J

detection limit of **BAA** for Fe^{3+} was determined to be 1.3 μM and 0.067 μM using UV-vis and fluorescence studies. Further, 2:1 binding mode between **BAA** and Fe^{3+} was observed from Job's plot measurements. In addition, the DFT calculation confirms the interaction mechanism between **BAA** and Fe^{3+}. Finally, the probe **BAA** has proven to be best suitable in real sample applications.

References

1 J. S. Kimand, D. T. Quang, *Chem. Rev.,* 2007, **107**, 3780-3799.

2 V. K. Gupta, N. Mergu and L. K. Kumawat, *Sens. Actuators, B* 2016, **223**, 101-113.

3 H. N. Kim, M. H. Lee, H. J. Kim, J. S. Kim and J. Yoon, *Chem. Soc. Rev.,* 2008, **37**, 1465-1472.

4 Y. W. Choi, G. J. Park, Y. J. Na, H. Y. Jo, S. A. Lee, G. R. You and C. Kim, *Sens. Actuators, B* 2014, **194**, 343-352.

5 M. A. Smith, P. L. Harris, L. M. Sayre and G. Perry, *Proc. Natl. Acad. Sci. U.S.A.,* 1997, **94**, 9866-8.

6 R. Bhowmick, A. S. M. Islam, U. Saha, G. S. Kumar and M. Ali, *New J. Chem.***,** 2018, **42**, 3435-3443

7 D. A. Weinstein, C. N. Roy, M. D. Fleming, M. F. Loda, J. I. Wolfsdorf, and N. C. Andrews, *Blood,* 2002, **100**, 3776-3781.

8 L. Huang, F. Hou, J. Cheng, P. Xi, F. Chen, D. Baiand Z. Zeng, *Org. Biomol. Chem.,* 2012, **10**, 9634-9638.

9 R. R. Crichton, S. Wilmet, R. Legssyer and R. J. Ward, *Inorg. J. Biochem.,* 2002, **91**, 9.

10 J. R. Burdo and J. R. Connor, *Biometals,* 2003,**16**, 63-75.

11 R. Evstatiev and C. Gasche, *Gut*, 2012, **61**, 933-952.

12 P. Aisen, M. Resnick and E. Leibold, *Curr. Opin. Chem. Biol.,* 1999, **3**, 200-206.

13 C. J. Earley, J. R. Connor, J. L. Beard, E. A. Malecki, D. K. Epstein and R. P. Allen, *Neurology,* 2000, **54**, 1698-1700.

14 D. Arch. *Biochem. Biophys.,* 2000, **373**, 1-6.

15 S. K. Sahoo, D. Sharma, R. K. Bera, G. Crisponi and J. F. Callan, *Chem. Soc. Rev.,* 2012, **41**, 7195-7227.

16 E. Beutler, *Blood Cells, Mol., Dis.,* 2007, **39**, 140-147.

View Article Online
DOI: 10.1039/C9NJ02655J

17 P. -F. Cheng, K. -X. Xu, W. Yao, E. Xie and J. Liu, *J. Lumin.,* 2013, **143**, 583–586.

18 C. F. Dick, A. L. A. Dos-santos and J. R. Meyer-Fernandes, *Biochim. Biophys. Acta,* 2014, **1840**, 2123-2127.

19 P. Xie, F. Guo, R. Xia, Y. Wang, D. Yao, G. Yang and L. Xie, *J. Lumin.,* 2014, **145**, 849-854.

20 S. J. Dixon and B. R. Stockwell, *Nat. Chem. Biol.,* 2013, **10**, 9-17.

21 J. R. Burdo and J. R. Connor, *BioMetals,* 2003, **16**, 63–75.

22 R. R. Crichton, D. T. Dexter and R. J. Ward, *Coord. Chem. Rev.,* 2008, **252**, 1189-1199.

23 H. Kozlowski, A. J. Klos, J. Brasun, E. Gaggelli, D. Valensin and G. Valensin, *Coord. Chem. Rev.,* 2009, **253**, 2665-2685.

24 F. B. E. Garah, C. Bijani, Y. Coppel, P. Faller and C. Hureau, *Inorg. Chem.,* 2011, **50**, 9024-9030.

25 E. Kopysc, K. Pyrzynska, S. Garbos and E. Bulska, *Anal. Sci.,* 2000, **16**, 1309–1312.

26 Z. Marczenko, Separation and Spectrophotometric Determination of Elements, Ellis Horwood, Chichester, 1986.

27 D. Karunasagar, J. Arunachalam and S. Gangadharan, *J. Anal. At. Spectrom.,* 1998, **13**, 679–682.

28 P. Ugo, L. Mortto, P. Bertoneell and J. Wang, *Electroanalysis,* 1998, **10**, 1017–1021.

29 J. C. Yu, J. M. Lo and K. M. Wai, *Anal. Chim. Acta,* 1983, **154**, 307–312.

30 C. Burrini and A. Cagnini, *Talanta,* 1997, **44**, 1219–1223.

31 A. Safawi, L. Eddon, M. Foulkes, P. Stockwell and W. Corns, *Analyst,* 1999, **124**, 185–189.

32 L. Bennun and J. Gomez, *Spectrochim. Acta, Part B,* 1997, **52**, 1195–1200.

33 Y. Yamini, N. Alizadeh and M. Shamsipur, *Anal. Chim. Acta,* 1997, **355**, 69–74.

34 A. S. Pithadia and M. H. Lim, *Curr. Opin. Chem. Biol.,* 2012, **16**, 67-73.

35 K. Bera, A. K. Das, M. Nag and S. Basak, *Anal. Chem.,* 2014, **86**, 2740-2746.

36 L. Zhou, X. Zhang, Q. Wang, Y. Lv, G. Mao, A. Luo and W. Tan, *J. Am. Chem. Soc.,* 2014, **136**, 9838-9841.

37 S. Sun, B. Qiao, N. Jiang, J. Wang, S. Zhang and X. Peng, *Org. Lett.,* 2014, **16**, 1132-1135.

38 A. Farhi, F. Firdaus and M. Shakir**,** *New J. Chem.***,** 2018, **42**, 6161-6167.

View Article Online
DOI: 10.1039/C9NJ02655J

39 M. Kumar, R. Kumar, V. Bhalla, P. R. Sharma, T. Kaur and Y. Qurishi, *Dalton Trans.,* 2012, **41**, 408-412.

40 P. Madhu and P. Sivakumar, *J. Photochem. Photobiol. A Chem.,* 2019, **371**, 341-348.

41 Yeung KS. Furans and Benzofurans. In: Gribble G. (eds) Metalation of Azoles and Related Five-Membered Ring Heterocycles. Topics in Heterocyclic Chemistry, 2012, 29. Springer, Berlin, Heidelberg.

42 G. S. Hassan, S. M. Abou-Seri, G. Kamel and M. M. Ali, *Eur. J. Med. Chem.,* 2014, **76**, 482–493.

43 K. V. Sashidhara, R. K.Modukuri, R. Sonkar, K. B. Rao and G. Bhatia, *Eur. J. Med. Chem.,* 2013, **68**, 38–46.

44 E. R. El-Sawy, M. S. Ebaid, H. M. Abo-Salem, A. G. Al-Sehemi and A. H. Mandour, *Arab. J. Chem.,* 2014, **7**, 914-923.

45 X. Jiang, W. Liu, W. Zhang, F. Jiang, Z. Gao and H. Zhuang, *Eur. J. Med. Chem.,* 2011, **46**, 3526–3530.

46 S. Shankerrao, Y. D. Bodke and S. Santoshkumar, *Arab. J. Chem.,* 2017, **10**, S554-S558.

47 C. Kirilmis, M. Ahmedzade, S. Servi, M. Koca, A. Kizirgil and C. Kazaz, *Eur. J. Med. Chem.,* 2008, **43**, 300–308.

48 K. M. Dawood, H. Abdel-Gawad, E. A. Rageb, M. Ellithey and H. A. Mohamed, *Bioorg. Med. Chem.,* 2006, **14**, 3672–3680.

49 L. Santana, M. Teijeira, E. Uriarte, C. Teran, B. Lin˜ ares and R. Villar, et al, *Eur. J. Pharm. Sci.,* 1999, **7**, 161–166.

50 J. Rangaswamy, H. V. Kumar, S. T. Harini and N. Naik, *Bioorg. Med. Chem. Lett.,* 2012, **22**, 4773–4777.

51 J. Rangaswamy, H. V. Kumar, S. T. Harini and N. Naik, *Arab. J. Chem.,* 2017, **10**, S2685-S2696.

52 Y. Malpani, R. Achary, S. Y. Kim, H. C. Jeong, P. Kim and S. B. Han, et al, *Eur. J. Med. Chem.,* 2013, **62**, 534–544.

53 S. A. Galal, A. S. Abd El-All, M. M. Abdallah and H. I. El-Diwani, *Bioorg. Med. Chem. Lett.,* 2009, **19**, 2420–2428.

54 K. Pisarewicz, D. Mora, F. C. Pflueger, G. B. Fields and F. Marl, *J. Am. Chem. Soc.,* 2005, **127**, 6207–6215.

View Article Online
DOI: 10.1039/C9NJ02655J

55 H. Wolosker, E. Dumin, L. Balan and V. N. Foltyn, *FEBS J.,* 2008, **275**, 3514–3526.

56 T. Zhou, R. C. Hider, P. Jenner, B. Campbell, C. J. Hobbs and S. Rose, et al, *Eur. J. Med. Chem.,* 2010, **45**, 4035–4042.

57 T. Zhou, R. C. Hider, P. Jenner, B. Campbell, C. J. Hobbs and S. Rose, *Bioorg. Med. Chem. Lett.,* 2013, **23**, 5279–5282.

58 P. J. Schechter, J. L. R. Barlow and A. Sjoerdsma, A clinical aspects of inhibition of ornithine decarboxylase with emphasis on therapeutic trials of eflornithine (DFMO) in cancer and protozoan diseases. In: P. P. Me Cann, A. E. Pegg, A. Sjoerdsma (Eds.), Inhibition of Polyamine Metabolism, New yourk: Acad. Press, Inc., 1987, 345–364.

59 A. Lavanya, R. Sribalan and V.Padmini, *J. Saudi Chem. Soc.,* **1**, 277-285.

60 H.A. Benesi and J.H. Hildebrand, *J. Am. Chem. Soc.,* 1949, **71**, 2703-2707.

61 P. Job, *Ann. Chim.,* 1928, **9**, 113-203.

62 T. Jovanovic, B. Stanovic and Z. Koricanac, *J. Pharm. Biomed. Anal.,* 1995, **13**, 213-217.

63 C. -Y. Li, C. -X. Zou, Y. -F. Li, J. -L. Tang and C. Weng, *Dyes Pigments,* 2014, **104**, 110-115.

64 A. K. Mahapatra, G. Hazra, N. K. Das, P. Sahoo, S. Goswami, H. –K. Fun, *J. Photochem. Photobiol. A,* 2011, **222**, 47-51.

65 J.A. Dean, Lang'es Handbook of Chemistry, McGraw-Hill, New York, 15thedn, 1999.

66 A. Jain, S. Wadhawan, V. Kumar and S.K. Mehta, *Chem. Phys. Lett.,* 2018, **706**, 53-61.

67 L. Wang, W. Li, W. Zhi, Y. Huang, J. Han, Y. Wang, Y. Ren and L. Ni, *Sens. Actuators B Chem.,* 2018, **260**, 243-254.

68 N. Narayanaswamy and T. Govindaraju, *Sens. Actuators B Chem.,* 2012, **161**, 304-310.

69 S. Devaraj, Y. -K. Tsui, C. -Y. Chiang and Y. -P. Yen, *Spectrochim. Acta, Part A,* 2012, **96**, 594–599.

70 S. D. Padghan, A. L. Puyad, R. S. Bhosale, S. V. Bhosale, S. V. Bhosale, *Photochem. Photobiol. Sci.***,** 2017, **16**, 1591-1595.

71 C. Kar, S. Samanta, S. Mukherjee, B. K. Datta, A. Ramesh and G. Das, *New J. Chem.***,** 2014, **38**, 2660-2669.

72 P. S. Nayab, M. Shkir, P. Gull, S. AlFaify, *J. Photochem. Photobiol. A,* 2017, **347**, 209-217.

View Article Online
DOI: 10.1039/C9NJ02655J

73 W. Zhu, L. Yang, M. Fang, Z, Wu, Q. Zhang, F. Yin, Q. Huang and C. Li, *J. Lumin.,* 2015, **158**, 38-43.